Rev. Roum. Sci. Techn.– Électrotechn. et Énerg.
Vol. **71**, *4*, pp. 495–500, Bucarest, 2026

ELECTRICAL CIRCUIT INFLUENCE ON THE RESPONSE OF STRUCTURALLY OPTIMIZED PIEZOELECTRIC HARVESTERS

CLAUDIA SĂVESCU[1,2], DANIEL COMEAGĂ[2], CRISTIAN NECHIFOR[1,*]

Keywords: Piezoelectric energy harvester; Structural optimization; Electrical circuit; Triangular cantilever; Finite element Analysis (FEA); Microelectromechanical systems (MEMS).

The paper investigates the influence of an electrical circuit on the electrical and mechanical behavior of structurally optimized piezoelectric energy harvesters. A quadmorph cantilever piezoelectric harvester comprising four PZT-5H active layers is analyzed. Structural optimization is pursued by reducing the piezoelectric material towards a triangular longitudinal section, comparing the performance with the original rectangular structure. Finite element simulations have been conducted, employing a digital twin with a full coupling of Solid Mechanics, Electrostatics, and Electrical Circuit physics interfaces. The electrical circuit emulates the finite input impedance of the spectrum analyzer used in the laboratory. Introducing the electrical impedance shifts the response parameters of interest in both mechanical and electrical domains, changing resonant frequency, stress, displacement, and voltage due to electromechanical coupling. The performance of the optimized structures is evaluated in terms of electrical response per unit volume of piezoelectric material under two relevant approaches: the same inertial mass and the same mechanical stress. The results demonstrate that the triangular structure enables a more efficient use of piezoelectric material, while significantly reducing material volume. The simulations with an electrical circuit indicate its potential use for fine-tuning.

1. INTRODUCTION

Piezoelectric technology offers broad potential as an alternative energy source for low-power applications, including industrial systems [1–3], or in actuation applications [4,5]. However, the technology has not reached maturity yet, and ongoing research continues to focus on improving electrical output and conversion efficiency through various optimization strategies [6–9]. Such optimization efforts are primarily driven by the need to improve the reliability and power-to-size ratio, enhancing electrical performance while reducing device dimensions and enabling more efficient use of active material. To this end, a variety of cantilever geometries have been investigated, including rectangular, triangular, trapezoidal, and other non-uniform profiles [10–13]. Finite element method (FEM) tools are widely employed to study these optimization approaches by systematically tailoring the shape and dimensions of piezoelectric harvesters [14].

Among the various piezoelectric architectures for energy harvesting, cantilever configurations remain widely adopted due to their high strain levels under base excitation and their suitability for low-frequency vibration environments. The mechanical geometry of the cantilever plays a critical role in determining strain distribution, stress concentration, resonant frequency, and electrical response [15].

Non-uniform geometries, including tapered and triangular profiles, have been shown to better align the distribution of active piezoelectric material with the stress profile of the cantilever, which is maximum near the clamped end and decreases towards the free tip. By reducing less active or weakly stressed material regions, such approaches can improve the electrical response normalized by material volume, while reducing overall material usage [16]. However, many studies evaluate these optimized geometries under idealized electrical boundary conditions, often assuming open-circuit or purely resistive loads.

In practical applications [1], the electrical load connected to a piezoelectric harvester is neither ideal [17] nor independent of the mechanical response. The finite electrical impedance of measurement instrumentation or interface circuitry interacts with the mechanical dynamics through electromechanical coupling, influencing resonant behavior, displacement amplitude, stress distribution, and electrical output. Neglecting this interaction can lead to discrepancies between numerical predictions and experimentally observed behavior, since measurement instrumentation influences sensitivity and system response.

The present work addresses this gap by investigating the combined influence of structural optimization and a realistic electrical circuit on the performance of a quadmorph cantilever piezoelectric energy harvester. A progressive reduction of the piezoelectric material toward a triangular longitudinal geometry is analyzed and compared against a conventional rectangular structure. The analyses are conducted using a fully coupled multiphysics finite element model, integrating the mechanical behavior, electrostatic response, as well as an external electrical circuit representing the finite input impedance of the measurement equipment used in the laboratory setup.

The structures' performance is evaluated using two complementary approaches: same inertial mass and same mechanical stress. These approaches enable an objective assessment of geometric and material efficiency under both mass-constrained and stress-constrained conditions.

2. PHYSICAL HARVESTER AND NUMERICAL MODEL

The structural optimization of a quadmorph cantilever piezoelectric energy harvester, starting from the Midé PPA-4011 harvester Fig. 1(a), is carried out, outlining the electrical circuit's influence. The quadmorph cantilever has the overall dimensions of 71 × 25.4 × 1.32 mm (L × W × H) and integrates four PZT-5H (lead zirconate titanate) layers with individual dimensions of 46 × 20.8 × 0.15 mm. Each piezoelectric layer is sandwiched between two copper electrodes with a thickness of 0.03 mm. Electrical insulation and mechanical protection are provided by five FR4 (flame-retardant type 4 glass-reinforced epoxy) layers, each 0.08 mm thick. Two FR4 layers are placed on the exterior, while the remaining three separate the four copper–PZT-5H–copper sandwiches to prevent electrical short-circuits between adjacent electrodes. Figure 1(b) presents a three-dimensional CAD model, as simulated, relying on the geometric data provided in the product datasheet [18].

[1] Romanian Research and Development Institute for Gas Turbines COMOTI, Bucharest, Romania.
[2] National University of Science and Technology Politehnica Bucharest, Romania.
E-mails: claudia.borzea@comoti.ro; daniel.comeaga@upb.ro; cristian.nechifor@comoti.ro (corresponding author).

DOI: 10.59277/RRST-EE.2026.4.3

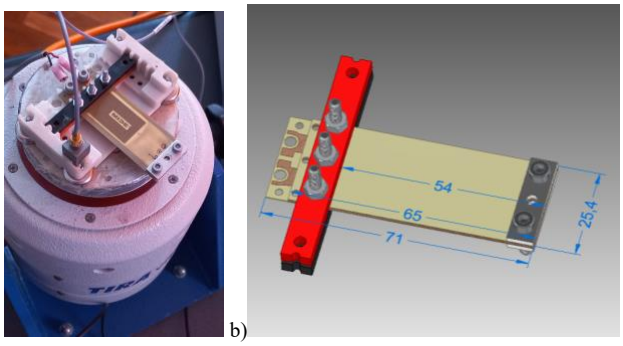


Fig. 1 – a) Midé PPA-4011 with 4 g tip mass; b) CAD model [16].

The numerical simulations were conducted in COMSOL Multiphysics 6.2, Fig. (2), using the finite element method (FEM). To evaluate both mechanical and electrical response, the Structural Mechanics – Piezoelectric Devices module was employed [19]. The electromechanical behavior was analyzed using a fully coupled multiphysics model integrating Solid Mechanics, Electrostatics, and Electrical Circuit interfaces, as follows:

- In the **Solid Mechanics** interface, the PZT-5H layers are defined as piezoelectric materials, and appropriate boundary conditions are applied. A base acceleration of 1 g (9.81 m/s²) is imposed on the lower clamping surface, consistent with the experimental conditions reported in one of our previous papers [20]. Mechanical damping is introduced as an isotropic loss factor of 0.0333, derived from the quality factor provided in the manufacturer's datasheet [18] and evaluated in [20].
- **The electrostatic** interface enforces charge conservation within the piezoelectric layers. Electrical terminals and ground are assigned to the piezoelectric faces, modeling the quadmorph as two bimorph-like pairs: the upper and lower pairs act in opposition, with the pairs connected in series and electrically in parallel.
- **The electrical circuit** interface connects the harvester terminals to an external load, allowing the evaluation of voltage, current, and electrical power. In all simulations, a parallel resistor–capacitor circuit (1 MΩ || 50 pF) is used to emulate the finite input impedance of the Stanford SR785 spectrum analyzer employed in the laboratory [16].

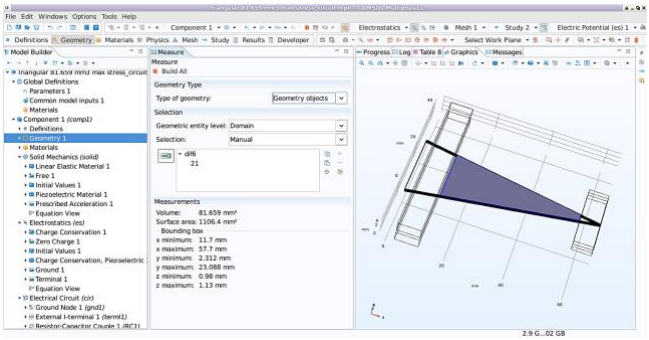


Fig. 2 – Simulation model showing piezoelectric layer measurement [16].

The frequency domain study yields slightly higher resonance frequencies than those obtained from modal analysis, with an offset of approximately 1 Hz. This offset results from the fact that the modal analysis does not consider the electrical problem, while the frequency domain study does account for the electromechanical coupling. For a system subjected to steady-state forced vibrations under an applied base acceleration, the frequency response is given by relation (1) [19]:

$$\omega_{acc} = \frac{\omega_n}{\sqrt{1-2\zeta^2}}, \tag{1}$$

where: ω_{acc} [rad/s] – pulsation (natural angular frequency); ω_n [rad/s] – undamped natural angular frequency; ζ [ND] – damping ratio.

The well-known relation (2) of the linear natural frequency, applicable to stratified composite structures, represents the computational base of the modal analysis [21].

$$f_n = \frac{\omega_n}{2\pi} = \frac{1}{2\pi}\sqrt{\frac{k}{m}} = \frac{1}{2\pi}\sqrt{\frac{3EI}{L^3}}, \tag{2}$$

where: f_n [Hz] – natural frequency; ω_n [rad/s] – natural pulsation; k [N/m] – equivalent stiffness constant of the composite beam; m [kg] – total beam mass; E [N/m^2] – equivalent elastic modulus; I [kg·m^2] – equivalent moment of inertia of beam's cross-section; L [m] – beam length.

Given the capacitive nature of piezoelectric structures, any external capacitance introduces a phase shift between current and voltage. However, since the operating resonant frequencies are significantly lower than the cutoff frequency imposed by the spectrum analyzer's impedance, the response is dominated by the resistive component, rendering the capacitive effect negligible, according to relation (3):

$$f_c = \frac{\omega_c}{2\pi} = \frac{1}{2\pi RC} = 3.183\ [\text{kHz}], \tag{3}$$

where: f_c [Hz] – cutoff frequency; ω_c [rad/s] – angular cutoff frequency; R [Ω] – load resistance (1 MΩ); C [F] – external capacitance (50 pF).

The piezoelectric constitutive relations couple the mechanical and electrical domains. In the numerical model, Solid Mechanics and Electrostatics are coupled via the Piezoelectric Effect multiphysics interface, enabling a simultaneous solution of the governing equations and piezoelectric constitutive relations. The strain–charge form was adopted, given by relation (4):

$$\begin{cases} \varepsilon_m = s^E\sigma + d^{\mathrm{T}}\mathbf{E}, \\ \mathbf{D} = d\sigma + \varepsilon_0\varepsilon_r^{\mathrm{T}}\mathbf{E}, \end{cases} \tag{4}$$

where: ε_m [ND] – strain; $s^{\boldsymbol{E}}$ [1/Pa] – elastic compliance, measured under constant electrical field conditions; σ [N/m^2] – mechanical stress; d [C/N] – piezoelectric charge constant; d^{T} [C/N] – piezoelectric charge constant, measured under constant stress; **E** [V/m] – electric field intensity; **D** [C/m^2] – electric displacement; ε_0 [F/m] – vacuum permittivity; $\varepsilon_r^{\mathrm{T}}$ [F/m] – relative permittivity, under constant stress.

Five cantilever geometries have been analyzed, starting from the original rectangular configuration and progressively reducing the tip material through three trapezoidal profiles, towards a triangular geometry. The overall beam length and cross-section of the piezoelectric layers at the clamped end are maintained the same for all cases. As illustrated in Fig. 3, the analyzed configurations are: (a) rectangular shape, 143.52 mm³; (b) wide-tip trapezoidal shape, 114.43 mm³ (-20.3% material); (c) medium-tip trapezoidal shape, 108.43 mm³ (-24.4% material); (d) narrow-tip trapezoidal shape, 100.70 mm³ (-29.8% material); and (e) triangular shape, 81.66 mm³ (-43.1% material).

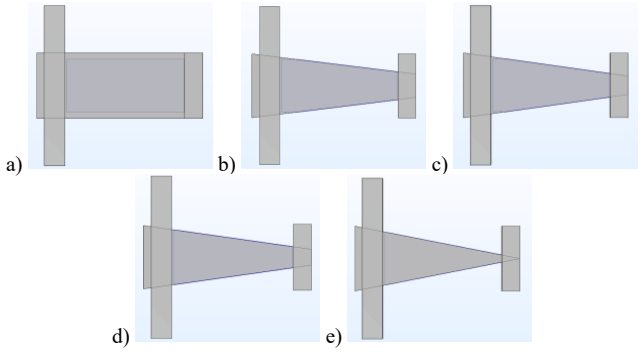


Fig. 3 – Simulated geometries: a) rectangular; b) wide tip trapezoidal; c) medium tip trapezoidal; d) narrow tip trapezoidal; e) triangular.

3. RESULTS AND DISCUSSION

3.1 SAME INERTIAL MASS

A first set of simulations was performed under identical inertial mass conditions, with a tip mass of 4 g. The geometry of the tip mass was defined to replicate the experimental configuration reported in the authors' previous work [20].

For the same inertial mass conditions, progressive reduction of the piezoelectric material toward the free tip leads to a gradual decrease in maximum mechanical stress, while the electrical response per unit volume increases. The triangular configuration exhibits the highest voltage output per unit volume of piezoelectric material. Including an electrical circuit affects both mechanical and electrical response parameters. Compared to idealized conditions, shifts in resonant frequency and variations in displacement and voltage response are observed, reflecting the influence of electromechanical coupling under electrical load.

Table 1 and Table 2 compare the considered piezoelectric beams with rectangular, trapezoidal, and triangular cross-sections under the same inertial mass conditions, with and without an electrical circuit. Increasing geometric taper results in a decrease in resonant frequency, and a decrease in von Mises stress is also observed. Although the rectangular beam produces the highest overall voltage per unit acceleration (Fig. 4), the triangular beam exhibits the highest voltage output per unit volume (Fig. 5). Overall, tapered geometries improve voltage generation efficiency per unit volume, at the same time reducing mechanical stress.

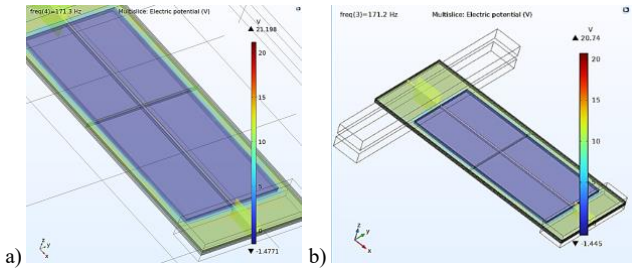


Fig. 4 – Electric potential at resonance for the rectangular cantilever: a) without electrical circuit; b) with electrical circuit.

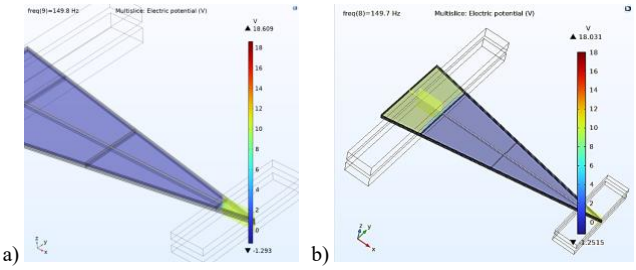


Fig. 5 – Electric potential at resonance for the triangular cantilever: a) without electrical circuit; b) with electrical circuit.

Table 1

Simulation results with the same inertial mass, without electrical circuit

No.	Cantilever section	Vol_{layer} [mm^3]	Vol_{piezo_total} [mm^3]	f_r [Hz]	w [mm]	σ_i [MPa]	V_{pk} [V/g]	V_{avg} [mV/mm^3]	P_r [mW/g]	P_{r_avg} [μW/mm^3]
1	Rectangular	143.52	574.08	171.3	0.565	80.07	21.198	36.925	–	–
2	Trapezoidal	114.43	457.72	158.6	0.501	45.26	16.308	35.629	–	–
3	Trapezoidal	108.43	433.72	162.1	0.496	34.85	17.783	41.001	–	–
4	Trapezoidal	100.7	402.80	152.3	0.519	28.24	17.093	42.435	–	–
5	Triangular	81.659	326.64	149.8	0.537	28.40	18.609	56.972	–	–

Table 2

Simulation results with the same inertial mass, with electrical circuit

No.	Cantilever section	Vol_{layer} [mm^3]	Vol_{piezo_total} [mm^3]	f_r [Hz]	w [mm]	σ_i [MPa]	V_{pk} [V/g]	V_{avg} [mV/mm^3]	P_r [mW/g]	P_{r_avg} [μW/mm^3]
1	Rectangular	143.52	574.08	171.2	0.554	78.5	20.740	36.127	0.404	0.704
2	Trapezoidal	114.43	457.72	158.5	0.492	44.39	16.597	36.260	0.250	0.546
3	Trapezoidal	108.43	433.72	162.0	0.485	34.06	17.353	40.010	0.273	0.629
4	Trapezoidal	100.7	402.80	152.2	0.507	27.60	17.199	42.699	0.270	0.670
5	Triangular	81.659	326.64	149.7	0.521	27.56	18.031	55.202	0.300	0.918

Under the same tip mass conditions, the maximum mechanical stress decreases progressively with geometric optimization. With the electrical circuit, we observe a reduction of approximately 65% for the triangular structure (27.56 MPa) compared to the rectangular cantilever (78.5 MPa). This indicates that comparable electrical output can be achieved at significantly lower stress levels, which may contribute to extended lifetime or allow the use of larger

inertial masses to further enhance the electrical response.

The results reported in the tables above are presented graphically in Fig. 6, progressing from the rectangular geometry to the triangular configuration through intermediate trapezoidal shapes. We plotted all parameters as a function of each structure's corresponding piezoelectric material volume. As expected, the voltage response and active power exhibit similar trends. The horizontal axes are displayed in reverse order to easily grasp and visualize the progressive stress reduction towards the triangular configuration. For the structures with the same tip mass of 4 g, with the electrical circuit, the voltage per unit volume of piezoelectric material increases by approximately 53%, from 36.127 mV/mm³ for the rectangular cantilever to 55.202 mV/mm³ for the triangular cutout geometry. Similarly, the power density at resonance increases by 30.4%, rising from 0.704 µW/mm³ to 0.918 µW/mm³.

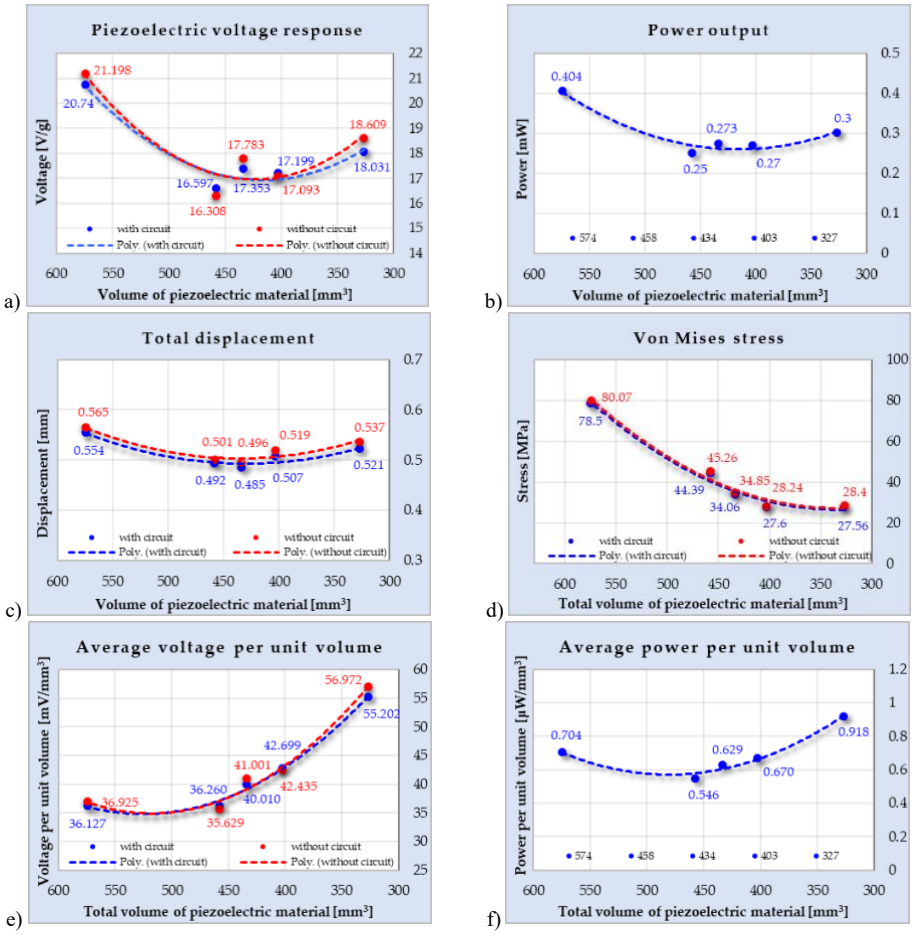


Fig. 6 – Graphs for the same inertial mass case, based on the numerical simulation results.

3.2 SAME MECHANICAL STRESS

Since the first set of simulations revealed a reduction in mechanical stress with geometric optimization, a second study was performed in which the maximum von Mises stress was maintained constant across all five configurations, as obtained for the rectangular structures. The reference stress, σ_{ref}, is ~80 MPa for no-load and 78.5 MPa for an added electrical circuit (Fig. 7).

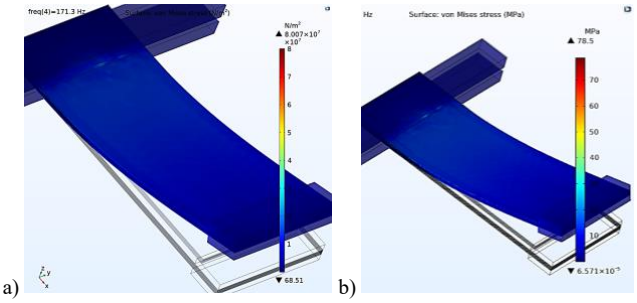


Fig. 7 – Stress at resonance: a) without; b) with electrical circuit.

This analysis is inherently more complex and computationally demanding, as mechanical stress does not scale linearly with the attached tip mass but depends on both the reduced geometry and the associated variation in the second moment of inertia.

Under identical stress conditions, the optimized geometries exhibit a substantial material efficiency increase, as shown in Table 3 and Table 4, whose data are plotted in the graphs in Fig. 8. In the case with a circuit, the displacement of the triangular structure reaches approximately three times that of the rectangular cantilever, because of the reduced bending stiffness. At the same time, the supported inertial mass increases approximately 3.3 times for the triangular configuration compared to the conventional rectangular beam. This leads to more than a 2.5-fold increase in voltage output and an almost 6.4-fold increase in the harvested power. The triangular cantilever exhibits a lower resonance frequency due to an increased supported mass compared to the rectangular configuration. Therefore, larger displacement amplitudes and higher voltage outputs are obtained, resulting in enhanced power.

Table 3
Simulation results with the same mechanical stress, without electrical circuit

No.	Cantilever section	Vol_{layer} [mm^3]	m_i [g]	σ_i [kg/m^3]	f_r [Hz]	w [mm]	σ_{i_ref} [MPa]	V_{pk} [V/g]	V_{avg} [mV/mm^3]	P_r [mW/g]	P_{r_avg} [μW/mm^3]
1	Rectangular	143.52	4	7850	171.3	0.565	80.07	21.198	36.925	–	–
2	Trapezoidal	114.43	8.7	17108	114.1	0.903	80.04	29.551	64.561	–	–
3	Trapezoidal	108.43	11.57	22750	101.4	1.164	80.09	41.956	96.735	–	–
4	Trapezoidal	100.7	14.34	28200	85.6	1.505	80.00	49.827	123.702	–	–
5	Triangular	81.659	12.94	25450	85.5	1.540	80.05	53.426	163.564	–	–

Table 4
Simulation results with the same mechanical stress, with electrical circuit

No.	Cantilever section	Vol_{layer} [mm^3]	m_i [g]	σ_i [kg/m^3]	f_r [Hz]	w [mm]	σ_{i_ref} [MPa]	V_{pk} [V/g]	V_{avg} [mV/mm^3]	P_r [mW/g]	P_{r_avg} [μW/mm^3]
1	Rectangular	143.52	4	7866	171.2	0.554	78.5	20.740	36.127	0.404	0.704
2	Trapezoidal	114.43	8.78	17262	113.6	0.886	78.5	30.032	65.612	0.872	1.905
3	Trapezoidal	108.43	11.81	23216.5	100.4	1.141	78.5	40.961	94.441	1.704	3.929
4	Trapezoidal	100.7	14.75	29000	84.5	1.475	78.5	50.208	124.647	2.551	6.333
5	Triangular	81.659	13.42	26400	84	1.510	78.5	52.172	159.725	2.580	7.899

The average electrical response normalized by the volume of piezoelectric material, while maintaining a constant maximum stress exhibits a great improvement in material efficiency: with electrical circuit, the voltage per unit volume increases by approximately 342%, from 36.127 mV/mm³ for the rectangular cantilever to 159.725 mV/mm³ for the triangular structure, Fig. 8(e). Similarly, the power density exhibits an increase of approximately 1022%, rising from 0.704 μW/mm³ to 7.899 μW/mm³ following material reduction, Fig. 8(f).

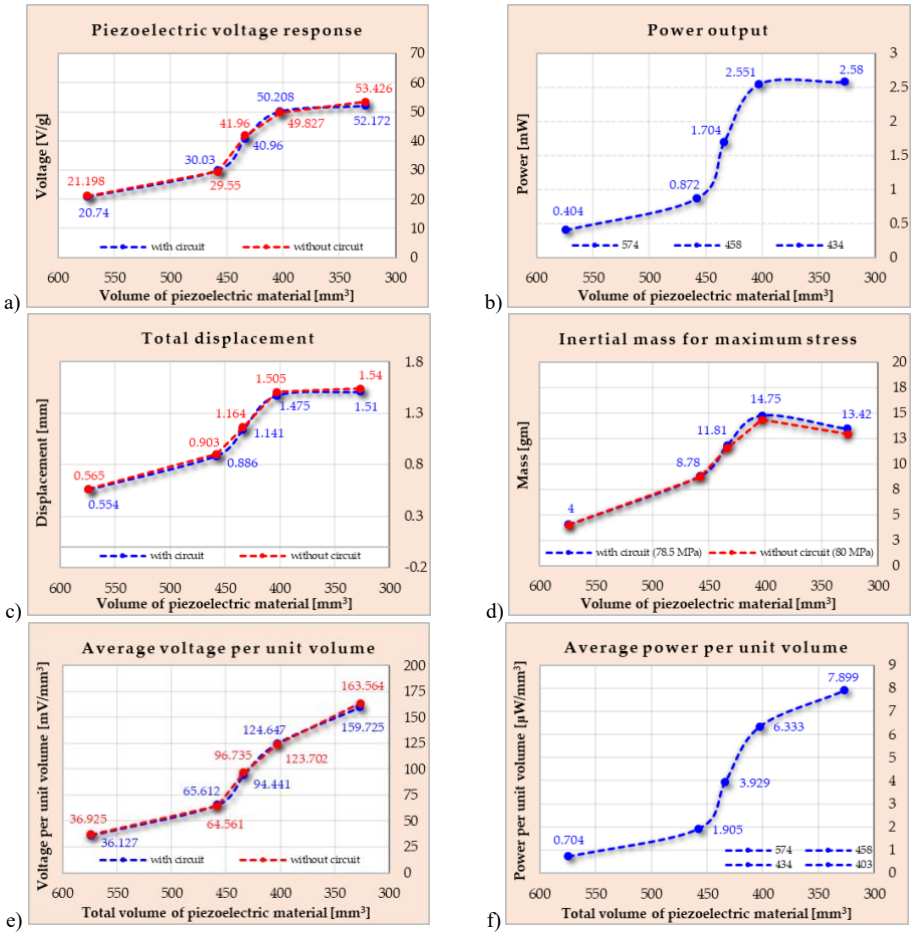


Fig. 8 – Graphs for the same mechanical stress case, based on the numerical simulation results.

4. CONCLUSIONS

The study analyses the influence of structural optimization and electrical circuit on the performance of a quadmorph cantilever piezoelectric energy harvester. Five geometries, ranging from a conventional rectangular profile, through three trapezoidal shapes, to a triangular longitudinal distribution of piezoelectric material, were analyzed using a fully coupled multiphysics finite element model.

The results demonstrate that reducing the piezoelectric material toward the free tip leads to a more efficient use of the active material. When effectiveness is evaluated per unit volume of piezoelectric material, the triangular configuration consistently exhibits the highest electrical response under both identical inertial mass and identical maximum stress conditions, while achieving a substantial material reduction.

Declaring an electrical circuit as the input impedance of the measurement equipment was shown to affect both mechanical and electrical response parameters. Compared to idealized conditions, shifts in resonant frequency and variations in displacement and voltage output were observed, highlighting the importance of accounting for electromechanical coupling under realistic electrical load.

The findings indicate that structural optimization and electrical circuit design must be considered jointly when assessing the performance of piezoelectric energy harvesters. Future work will focus on the integration of dedicated energy harvesting interface circuits to evaluate their impact on power extraction and system-level performance.

ACKNOWLEDGEMENTS

This work is part of "National Platform for Semiconductor Technologies (PNTS)", SMIS code 351364, carried out with the support of the Romanian Ministry of Investments and European Projects, through the Smart Growth, Digitalization and Financial Instruments Program 2021-2027 (PoCIDIF), co-financed by the European Regional Development Fund.

The research is supported by NRDI for Gas Turbines COMOTI, under the "Nucleu" Program within the Romanian Research, Development, and Innovation Plan 2022-2027, supported by the Romanian Ministry of Research, Innovation, and Digitalization, contract 31N/2023, project PN 23.12.09.

CREDIT AUTHORSHIP CONTRIBUTION STATEMENT

Claudia SĂVESCU: Conceptualization, formal analysis, investigation, numerical simulations, methodology, data curation, validation, visualization, writing.

Daniel COMEAGĂ: Formal analysis, conceptualization, methodology, validation, supervision.

Cristian NECHIFOR: Formal analysis, investigation, methodology.

Received on 29 May 2026

REFERENCES

1. C. Săvescu, D. Comeagă, M. Roman, D. Lale, R. Stoica, E. Vasile, C. Nechifor, A. Stoicescu, "Experimental study of a piezoelectric harvester vibrating on an industrial screw compressor," Rev. Roum. Sci. Techn. – Électrotechn. et Énerg., **70**, *1*, pp. 9–14 (2025).
2. C. Săvescu, V. Petrescu, D. Comeagă, I. Vlăducă, C. Nechifor, F. Niculescu, "Vibration analysis of a twin-screw compressor as a potential source for piezoelectric energy harvesting," Rev. Roum. Sci. Techn. – Électrotechn. et Énerg., **68**, *3*, pp. 253–258 (2023).
3. C. Săvescu, D. Comeagă, A. Morega, Y. Veli, "Experimental tests with piezoelectric harvester for tuning resonant frequency to vibrating source," Rev. Roum. Sci. Techn. – Électrotechn. et Énerg., **67**, *4*, pp. 457–460 (2022).
4. A. Ounissi, A. Kaddouri, M.-S. Aggoun, R. Abdessemed, "Second order sliding mode controllers of micropositioning stage piezoelectric actuator with Colman-Hodgdon model parameters," Rev. Roum. Sci. Techn. – Électrotechn. et Énerg., **67**, *1*, pp. 41–46 (2022).
5. R.G. Ballas, "Piezoelectric bending transducers: the physics of their static and dynamic behavior: a textbook about indispensable actuators in microtechnology, mechatronics and medical technology," Springer, Berlin, Heidelberg (2025).
6. S. De Caro, R. Montanini, S. Panarello, A. Quattrocchi, T. Scimone, A. Testa, "A PZT-based energy harvester with working point optimization," 6th International Conference on Clean Electrical Power (ICCEP), pp. 699–704 (2017).
7. M. Ashford, B. Onyenucheya, J. Zirnheld, K. Burke, "Improving a piezoelectric energy harvester output using a synchronized switch harvesting design," IEEE Pulsed Power Conference (PPC), pp. 1–5 (2021).
8. D. Zhu, S. Beeby, J. Tudor, N. White, N. Harris, "Improving output power of piezoelectric energy harvesters using multilayer structures," Procedia Engineering, **25**, pp. 199–202 (2011).
9. A. Pasharavesh, H. Dalir, "Flexural modes coupling in cantilever-type piezoelectric energy harvesters," Energy Reports, **7**, pp. 6438–6450 (2021).
10. D. Benasciutti, L. Moro, S. Zelenika, E. Brusa, "Vibration energy scavenging via piezoelectric bimorphs of optimized shapes," Microsystem Technologies, **16**, *5*, pp. 657–668 (2010).
11. V.J. Caetano, M.A. Savi, "Multimodal pizza-shaped piezoelectric vibration-based energy harvesters," Journal of Intelligent Material Systems and Structures, **32**, *20*, pp. 2505–2528 (2021).
12. P. Skėrys, R. Gaidys, "A dynamic analysis of a cantilever piezoelectric vibration energy harvester with maximized electric polarization due to the optimal shape of the thickness for first eigen frequency," Applied Sciences, **15**, *13*, Art. no. 7525 (2025).
13. V. Hassani, T. Tjahjowidodo, "Structural response investigation of a triangular-based piezoelectric drive mechanism to hysteresis effect of the piezoelectric actuator," Mechanical Systems and Signal Processing, **36**, *1*, pp. 210–223 (2013).
14. C. Borzea, D. Comeagă, Y. Veli, A. Săvescu, "Piezoelectric cantilever harvester with trapezoidal/triangular section for increased conversion efficiency," Iberian COMSOL Multiphysics Conference 2022, pp. 54–57 (2022), https://www.researchgate.net/publication/363710805_Piezoelectric_Cantilever_Harvester_with_TrapezoidalTriangular_Section_for_Increased_Conversion_Efficiency.
15. J. Erhart, P. Půlpán, M. Pustka, "Piezoelectric ceramic resonators," Springer International Publishing, Cham (2017).
16. C. Săvescu, D. Comeagă, A. Stoicescu, "Optimization of cantilever piezoelectric harvester to triangular shape with material reduction using finite element analysis," Heliyon, **10**, *13*, Art. no. e33209 (2024).
17. C. Săvescu, D. Comeagă, M. Roman, A. Stoicescu, C. Nechifor, M. Beldiman, "Maximizing the power output of a piezoelectric harvester by optimal resistive load," 14th International Symposium on Advanced Topics in Electrical Engineering (ATEE) (2025).
18. Midé Technology, "PPA products datasheet & user manual." https://cdn2.hubspot.net/hubfs/3841176/Data-Sheets/ppa-piezo-product-datasheet.pdf (2017).
19. COMSOL, "Structural mechanics module user's guide." https://doc.comsol.com/6.1/doc/com.comsol.help.sme/StructuralMechanicsModuleUsersGuide.pdf (2022).
20. C. Borzea, D. Comeagă, A. Săvescu, "Boosting the electric output of a cantilever piezoelectric harvester by tip curvature blocking elements," 8th European Conference on Renewable Energy Systems (ECRES 2020), pp. 344–350 (2020), https://www.researchgate.net/publication/348370037_Boosting_the_Electric_Output_of_a_Cantilever_Piezoelectric_Harvester_by_Tip_Curvature_Blocking_Elements
21. C. Borzea, D. Comeagă, "Reliability of Euler-Bernoulli model for multilayer composite piezoelectric beams," 11th International Symposium on Advanced Topics in Electrical Engineering (ATEE) (2019).